Precipitation-driven gamma radiation enhancement over the Atlantic Ocean

Susana M Barbosa[1], Nuno Dias[1], Carlos Almeida[1], Guilherme Amaral Silva[1], António Ferreira[1], António Camilo[2], and Eduardo Silva[1]

[1]INESC TEC
[2]Marinha

February 27, 2023

Abstract

Gamma radiation over the Atlantic Ocean Gamma radiation over the Atlantic Ocean was measured continuously from January to May 2020 by a NaI(Tl) detector installed on board the Portuguese navy's ship NRP Sagres. Enhancements in the gamma radiation values are identified automatically by an algorithm for detection of anomalies in mean and variance as well as by visual inspection. The anomalies are typically +50% above the background level and relatively rare events (˜ < 10% of the days). All the detected anomalies are associated with simultaneous precipitation events, consistent with the wet deposition of scavenged radionuclides. The enhancements are detected in the open ocean even at large distances (+ 500 km) from the nearest coastline. Back trajectories reveal that half of these events are associated with air masses experiencing continental land influences, but the other half don't display evidence of recent land contact. The enhancements in gamma radiation very far from land and with no evidence of continental fetch from back trajectories are difficult to explain as resulting only from radionuclides with a terrestrial source such as radon and its progeny. Further investigation and additional measurements are needed to improve understanding on the sources of ambient radioactivity in the open ocean and assess whether gamma radiation in the marine environment is influenced not only by radionuclides of terrestrial origin, but also cosmogenic radionuclides, like Beryllium-7, formed in the upper atmosphere but with the ability to be transported downward and serve as a tracer of the aerosols to which it attaches.

Precipitation-driven gamma radiation enhancement over the Atlantic Ocean

Susana Barbosa[1], Nuno Dias[1], Carlos Almeida[1], Guilherme Silva[1], António Ferreira[1], António Camilo[2], Eduardo Silva[1]

[1]INESC TEC - INESC Technology & Science, Porto, Portugal
[2]CINAV, Marinha, Lisboa, Portugal

Key Points:

- Precipitation-driven enhancements in gamma radiation are detected in the oceanic environment.
- Gamma radiation enhancements are found in the open ocean at large distances (+ 500 km) from the nearest coastline.
- Rain events do not produce enhancements in gamma radiation, even close to the coast, for marine air masses with no recent contact with land.

Corresponding author: Susana Barbosa, `susana.a.barbosa@inesctec.pt`

Abstract

Gamma radiation over the Atlantic Ocean was measured continuously from January to May 2020 by a NaI(Tl) detector installed on board the Portuguese navy's ship NRP Sagres. Enhancements in the gamma radiation values are identified automatically by an algorithm for detection of anomalies in mean and variance as well as by visual inspection. The anomalies are typically +50% above the background level and relatively rare events ($\sim<$ 10% of the days). All the detected anomalies are associated with simultaneous precipitation events, consistent with the wet deposition of scavenged radionuclides. The enhancements are detected in the open ocean even at large distances (+ 500 km) from the nearest coastline. Back trajectories reveal that half of these events are associated with air masses experiencing continental land influences, but the other half don't display evidence of recent land contact. The enhancements in gamma radiation very far from land and with no evidence of continental fetch from back trajectories are difficult to explain as resulting only from radionuclides with a terrestrial source such as radon and its progeny. Further investigation and additional measurements are needed to improve understanding on the sources of ambient radioactivity in the open ocean and assess whether gamma radiation in the marine environment is influenced not only by radionuclides of terrestrial origin, but also cosmogenic radionuclides, like Beryllium-7, formed in the upper atmosphere but with the ability to be transported downward and serve as a tracer of the aerosols to which it attaches.

Radioactive elements such as the noble gas radon and those produced by its radioactive decay are naturally present in the environment and used as tracers of atmospheric transport and composition. In particular the noble gas radon, being inert and of predominantly terrestrial origin, is used to identify pristine marine air masses with no land contamination. Precipitation over land typically brings radon from the atmosphere to the surface, enhancing gamma radiation on the ground, but over such enhancements have not been identified before nor expected over the ocean due the low amount of radon typical of marine air masses. Here we report, for the first time, gamma radiation enhancements associated with precipitation in the oceanic environment, using measurements performed over the Atlantic ocean in a campaign onboard the Portuguese navy sip NRP Sagres.

1 Introduction

Gamma radiation is well known to exhibit significant enhancements associated with precipitation events (e.g. Fujinami (1996); Yakovleva et al. (2016); Bossew et al. (2017); Melintescu et al. (2018)). The increase in gamma radiation results mainly from the wet deposition of the progeny of Rn-222 (radioactive half-life = 3.82 days), mainly Pb-214 and Bi-214 (e.g. Livesay et al. (2014); Bottardi et al. (2020); Zelinskiy et al. (2021)). The gamma radiation peaks typically exhibit a short time rise and a longer decrease time resulting from the direct deposition of Pb-214 and Bi-214 on the ground and subsequent decay, with gamma radiation remaining above background values for several half-lives, about 3-4 hours (Fujitaka et al., 1992; Greenfield et al., 2008; Livesay et al., 2014; Reuveni et al., 2017). The concentration of radon progeny in precipitation is not correlated with the concentration of radon progeny in air near the surface (Fujinami, 1996), suggesting that the scavenging of radionuclides to the ground is dominated by processes within the clouds - nucleation scavenging and interstitial aerosol collection by cloud or rain droplets - rather than by processes below the cloud base (e.g. Takeuchi and Katase (1982); Paatero and Hatakka (1999)). The increase in gamma radiation associated with precipitation depends on the history of the corresponding contributing air mass (Paatero, 2000; Inomata et al., 2007; Mercier et al., 2009; S. Barbosa et al., 2017) but no clear association has been found between precipitation (intensity, amount and duration), and the resulting enhancement in gamma radiation (Fujinami, 1996; Burnett et al., 2010; Cortes et al., 2001; Greenfield et al., 2003; Datar et al., 2020). The connection between the temporal variability of gamma radiation and precipitation is not straightforward as a result of the complex interplay of factors such as the amount and intensity of precipitation, the cloud's thickness and base height, and the atmospheric concentration of sub-micron aerosols, all influencing the scavenging of radon progeny (e.g. S. Barbosa et al. (2017)).

Although gamma radiation peaks driven by precipitation have been studied in numerous and varied settings, here we report, for the first time, gamma radiation enhancements associated with precipitation in the oceanic environment. Measurements of total gamma radiation have been performed in open ocean over the North and South Atlantic in the framework of project SAIL - Space-Atmosphere-Ocean Interactions in the marine boundary Layer (S. Barbosa, Dias, et al., 2022), in a field campaign inspired by the Carnegie expedition and its contribution to understanding the global atmospheric electric field (Harrison, 2013, 2020).

Over the ocean radon exhalation from the surface is negligible. The total oceanic contribution to radon in the global atmosphere is only about 2% of all radon exhaled from continents (Wilkening & Clements, 1975). Using a gas transfer model, Schery and Huang (2004) derived an oceanic radon flux of 0.00182 atom $cm^{-}2$ $s^{-}1$, with the model indicating strong spatial variability associated to its dependence on surface wind speed. Emission of radon from the ocean was taken by B. Zhang et al. (2021) as 0.005 atom $cm^{-}2$ $s^{-}1$, 200 times less than land emissions. The negligible oceanic contribution enables radon to be used as an unambiguous indicator of recent terrestrial influence on an air mass (e.g. Wilkening (1981); Balkanski et al. (1992)) and many studies have used radon to identify continental fetch areas and long-range transport from terrestrial source regions (e.g. Polian et al. (1986); Zahorowski et al. (2005); Chambers et al. (2013, 2018); Jun et al. (2022)).

Unlike radon, which is inert and neutral, radon progeny are mostly positively charged and react with water vapor and trace gases, forming clusters of small particles that are quickly and irreversibly attached to existing aerosols in the atmosphere (Whittlestone, 1990; Postendorfer et al., 1994; Bigg, 1996; Porstendörfer, 2001; Elsässer et al., 2011). Therefore the fate of gamma-emitting radon progeny, after their formation by radioactive decay, is closely linked to that of aerosols, particularly accumulation mode aerosol particles with a diameter of a few hundred nanometers (Paatero et al., 2017). Observations of aerosol concentration over the ocean are limited, but deposition of aerosols to the surface ocean, particularly the open ocean away from continental land masses, is an important phenomena affecting marine biogeochemical cycles (e.g. Wei et al. (2022)). Radioactive aerosols of radon progeny are deposited onto the Earth's surface primarily by precipitation as accumulation-mode aerosols are too small for gravitational settling and too large to be deposited by Brownian motion (F. Zhang et al., 2021).

In a marine setting gamma radiation variability mainly reflects atmospheric rather than surface contributions. In terms of surface sources, gamma emission from the ocean by radon degassing is negligible. The contribution from terrestrial sources containing uranium and thorium and their decay series, which is substantial over land, is reduced over the ocean. Gamma radiation from radionuclides in ocean sediments is attenuated by water and doesn't reach the surface. In sea water potassium (K-40 isotope) is the dominant gamma-emitting radionuclide, but it has a fairly uniform geographic distribution (Solomon, 1988). In terms of atmospheric contributions, these include secondary cosmic radiation, gamma rays resulting from the interaction of cosmic rays with gas molecules in the atmosphere (e.g. Wissmann et al. (2005); Mertens (2016)), and airborne radionuclides. Airborne gamma-emitting elements include radon progeny (short-lived Pb-214, Bi-214 and long-lived Pb-210) and cosmogenic radionuclides such as Be-7 (e.g. Bossew et al. (2017); European Commission (2019)).

In the present study we document enhancements in gamma radiation over the Atlantic ocean from high-resolution gamma radiation measurements. The data are described in section 2, the analysis is detailed in section 3 and concluding remarks are provided in section 4.

2 Data

Data considered in this study consist of gamma radiation (section 2.1) and meteorological measurements (section 2.2) performed over the Atlantic ocean from January to May 2020 on board the sail ship NRP Sagres. Figure 1 shows the map of the ship's trajectory since its departure from Lisboa in January 5th 2020. The trip was initially planned to last for 371 days, but was interrupted due to the COVID-19 pandemic and subsequent restrictions in port activities. On March 25th the ship arrived to Cape Town for refueling and supplies, departing the same day back to Portugal, instead of resuming the trip into the Indian Ocean as originally planned. The ship arrived to Lisboa on May 10th, after a stop for repairs at the port of Praia, Cape Verde. Overall data completion is $> 95\%$, with two short periods of data loss due to issues in the onboard computer and storage systems, which occurred on March 8th and 9th (during the trip from Buenos Aires to Cape Town) and then from 4 to 6 April, in the leg from Cape Town to Lisboa.

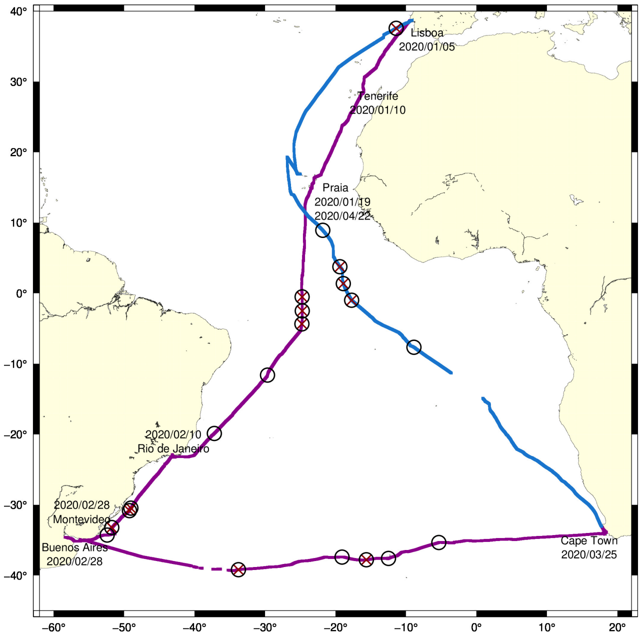

Figure 1. Map of the trajectory of NRP Sagres ship. The data points represented by light blue correspond to the Lisboa - South Africa leg of the trip, and darker blue represents the return trip from South Africa to Lisboa. The symbols ◯ mark the location of the rain events listed in Table S1 and symbols × represent the location of the gamma anomalies listed in table 1. Blanks denote points with no available data due to computer issues ($<$ 5% of the total data collected).

2.1 Gamma radiation data

Gamma measurements are performed with a 3”×3” (76×76 mm) NaI(Tl) cyllindrical scintillator (Scionix, the Netherlands) equipped with an electronic total count single channel analyzer for acquiring total counts of gamma radiation in the 475 keV to 3 MeV energy range. The selection of this energy range enables the reduction of Compton background in the 50–475 keV low-energy range, improving the sensitivity of short-lived radon progeny measurements (Zafrir et al., 2011). The NaI(Tl) scintillator is encased in a water-proof container designed for underwater measurements, in order to protect the instrument from harsh marine conditions. The sensor is installed on the mizzen mast of the ship, at a height of $\sim$ 20 m, in an upright position and pointing upwards. Counts are acquired at a sampling rate of 1-second and further aggregated into counts per minute. Further details on data management and pre-processing are described in the SAIL project's data management plan (S. Barbosa & Karimova, 2021).

The 1 minute time series of gamma radiation counts is presented in Figure 2. Except for the evident ocean-land contrast, the temporal variation of gamma radiation counts is small, being more prominent in the first month of the series and very stable afterwards. The long-term component of gamma radiation variability is estimated by robust local regression (Cleveland et al., 1992) and represented by the colored solid line in Figure 2. The measurements performed over land during the stops of the ship along its journey, represented in gray in Figure 2 (top), are not further considered, as this work focus only on the observations of gamma radiation over the ocean. Thus the gamma radiation time series considered hereafter, displayed in Figure 2 (bottom), consists of the 1-minute gamma radiation counts measured exclusively in the marine environment (126 days in total).

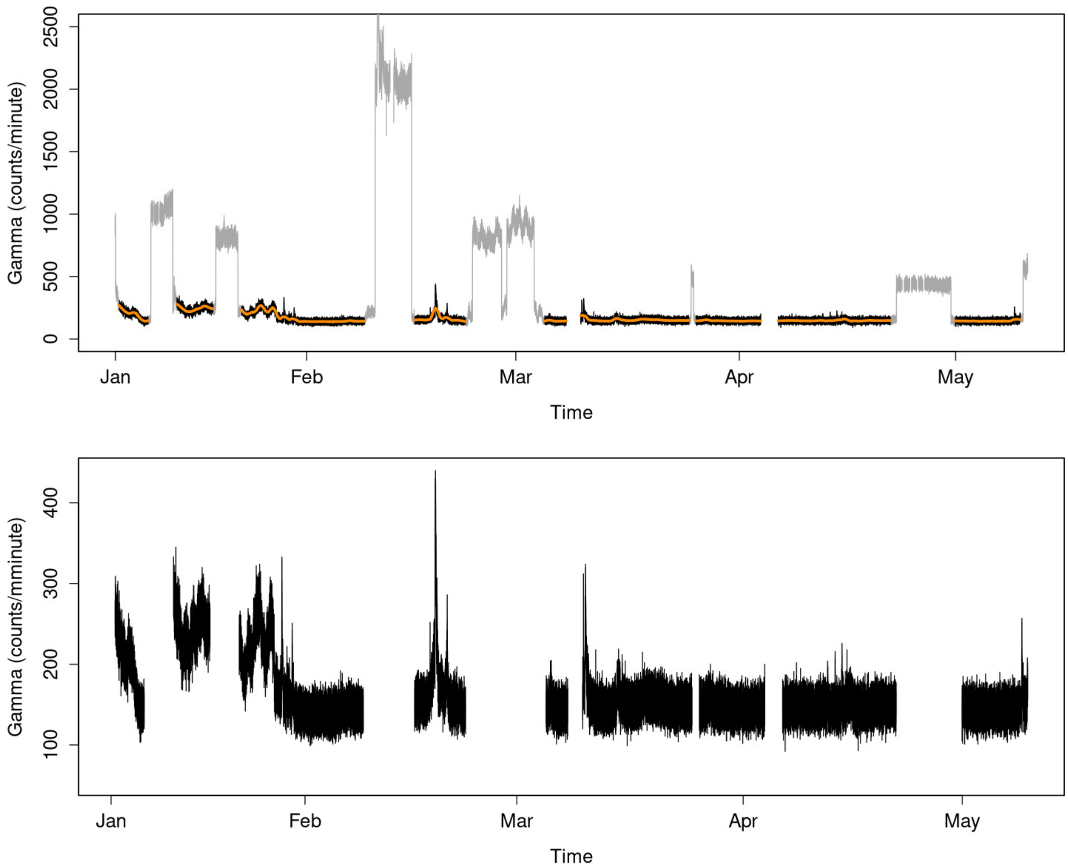

Figure 2. Time series of gamma radiation data. Top: complete 1-minute series with land measurements represented in gray and long-term variability by the solid colored line. Bottom: time series of marine-only 1-minute gamma radiation counts.

2.2 Meteorological data

Two distinct types of meteorological data are available from the SAIL campaign: automatic data collected by sensors, with no need of human intervention, and data collected by human observers. The meteorological optical range is measured every 1-minute

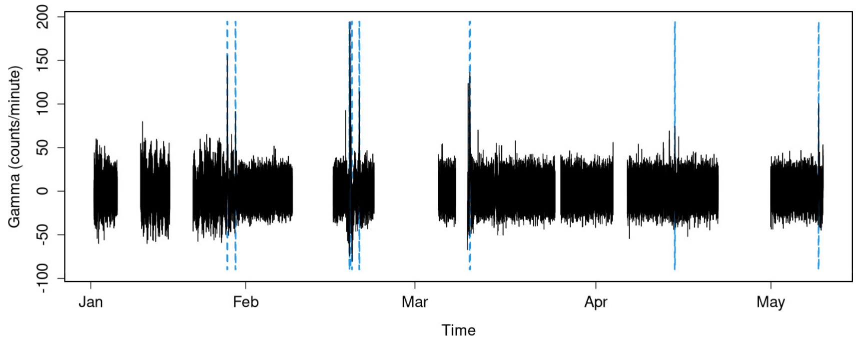

Figure 3. Detrended time series of gamma radiation. The anomalies identified by the CAPA algorithm are represented by the vertical dashed lines.

by a visibility sensor SWS050 (Biral, UK) providing measurements in the range from 10m to 40 km. The visiblity sensor is located at the same height and on the same mast as the gamma radiation instrument. Rain, and basic meteorological parameters such as atmospheric pressure, temperature and wind, are collected in a non-automatic way by the ship's crew every 1-hour as part of the navy's operational routine during navigation (no meteorological information is available when the ship is docked). Rainfall events are recorded in a qualitative way (drizzle $<$ light $<$ moderate). The geographic location of rain events is shown as $\bigcirc$ in Figure 1. Table S1 summarizes the available information in terms of rain occurrences during the whole trip. In general rain was not a frequent event, as it is registered in only 16 days out of a total of 126. Times were originally recorded as local time but are presented as coordinated universal time (UTC), as for all the other data. Rain registered at a given hour corresponds to rain observed within the previous hour.

3 Analysis

3.1 Detection of gamma radiation anomalies

For the detection of anomalies in the marine gamma radiation time series (Fig. 2, bottom), two complementary distinct approaches are used: an automatic method and visual inspection of the time series. The automatic detection of anomalies is performed using the Collective And Point Anomaly (CAPA) algorithm (Fisch et al., 2022). The outcomes of the algorithm are very much dependent on the pre-processing of the time series in terms its standardization and handling of missing values. This is particular critical in this case due to the numerous gaps in the time series. Thus for the application of the CAPA procedure the following pre-processing steps are taken: i) the long-term variability signal (represented by the solid line in Fig. 2 top) is subtracted from the series for stabilization of the mean; and ii) the gaps are filled by replacing the missing values by values resulting from a normal distribution with the same mean and variance as the gamma radiation time series. The CAPA algorithm is then applied to the pre-processed time series using a penalty for control of false positives of $2\times\frac{1+\phi}{1-\phi}log(n)$, where ϕ is set as 0.9 and n is the length of the time series. The results are displayed in Figure 3. In a conservative approach (mainly determined by the penalty value for control of false positives), a total of 8 anomalies are detected. Visual inspection confirms these, and further identifies 4 additional candidate anomalies in gamma radiation, summarized in Table 1. The geographic location of these 12 anomalies is displayed in Figure 1.

Table 1. Anomalies identified in the marine gamma radiation observations by visual inspection and by using the CAPA algorithm. It is also indicated whether these periods identified as anomalous correspond to rain events or anomalies in visibility.

date	time (UTC)	Visual detection	CAPA algorithm	Rain	Visibility
2020-01-28	19:00-21:00	✓	✓	✓	✓
2020-01-29	13:00-14:00	✓	-	✓	✓
2020-01-30	05:00-07:00	✓	✓	✓	✓
2020-02-18	19:00-24:00	✓	✓	✓	✓
2020-02-19	01:00-02:00	✓	✓	-	✓
2020-02-20	10:00-12:00	✓	✓	-	✓
2020-03-10	08:00-16:00	✓	✓	✓	✓
2020-03-15	10:00-11:00	✓	-	-	✓
2020-04-12	14:00-16:00	✓	-	✓	✓
2020-04-13	14:30-15:30	✓	-	-	✓
2020-04-14	13:00-14:00	✓	✓	✓	✓
2020-05-09	04:00-06:00	✓	✓	✓	✓

Table 2. Contingency table for the number of occurrences (in days) of rain and gamma radiation anomalies.

	number of days rain	number of days no rain	
gamma anomaly	8	4	12
no gamma anomaly	8	106	114
	16	110	126

3.2 Characteristics of marine gamma anomalies

Table 2 summarizes the occurrence of anomalies in the gamma radiation time series as a function of the rainfall information. From a total of 126 days with gamma radiation measurements over the ocean, gamma anomalies are identified in only 12 days ($< 10\%$). Most of these anomalies ($\sim 65\%$) are associated with the occurrence of rain according to the available meteorological information from human observers. They are also associated with concurrent anomalies in the meteorological optical range from the visibility sensor, as illustrated in Figure 4. Only 4 gamma radiation anomalies occur in days for which rain was not registered by human observers. And in all these 4 cases the anomalies in gamma radiation are associated with simultaneous sharp drops in visibility, as shown in Figure 5. Thus it seems likely that also these gamma radiation anomalies are driven by precipitation which apparently failed to be registered by the human observers.

Although all enhancements in gamma radiation are associated with the occurrence of precipitation, the reverse is not true, i.e. the occurrence of precipitation is not necessarily associated with an anomaly in gamma radiation. For a total of 16 days with registered rain events, half do not have a corresponding anomaly in the gamma radiation counts. These cases are detailed in Figures 6 and 7. Comparison of the visibility measurements with the meteorological information in Table S1 shows strong consistency between human-recorded and instrumental information. Only in one case (16th April 2020 - Figure 7) the visibility data does not point to the occurrence of rain, in disagreement with the qualitative information of early morning drizzle. In all the remaining cases vis-

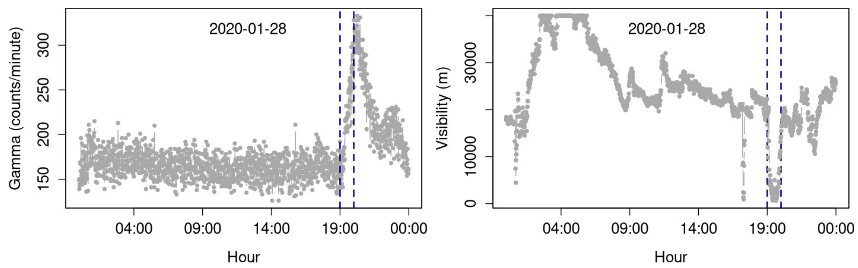

Figure 4. Detail (28th January 2020) of 1-minute time series of gamma radiation counts (left) and visibility (right). The vertical dashed lines represent the period of occurrence of moderate rain as indicated in the available meteorological information.

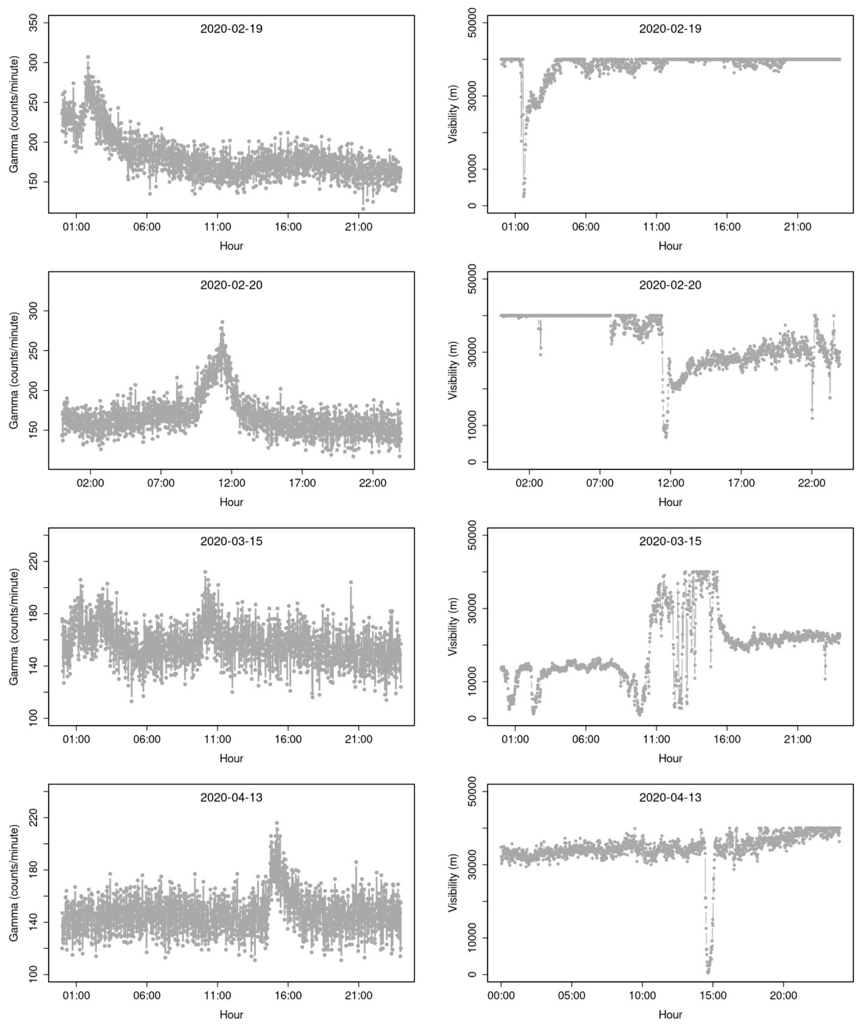

Figure 5. Detail of 1-minute time series of gamma radiation counts (left) and visibility (right) for the days in which an anomaly is identified in gamma radiation but rain is not registered in the navy's meteorological observations.

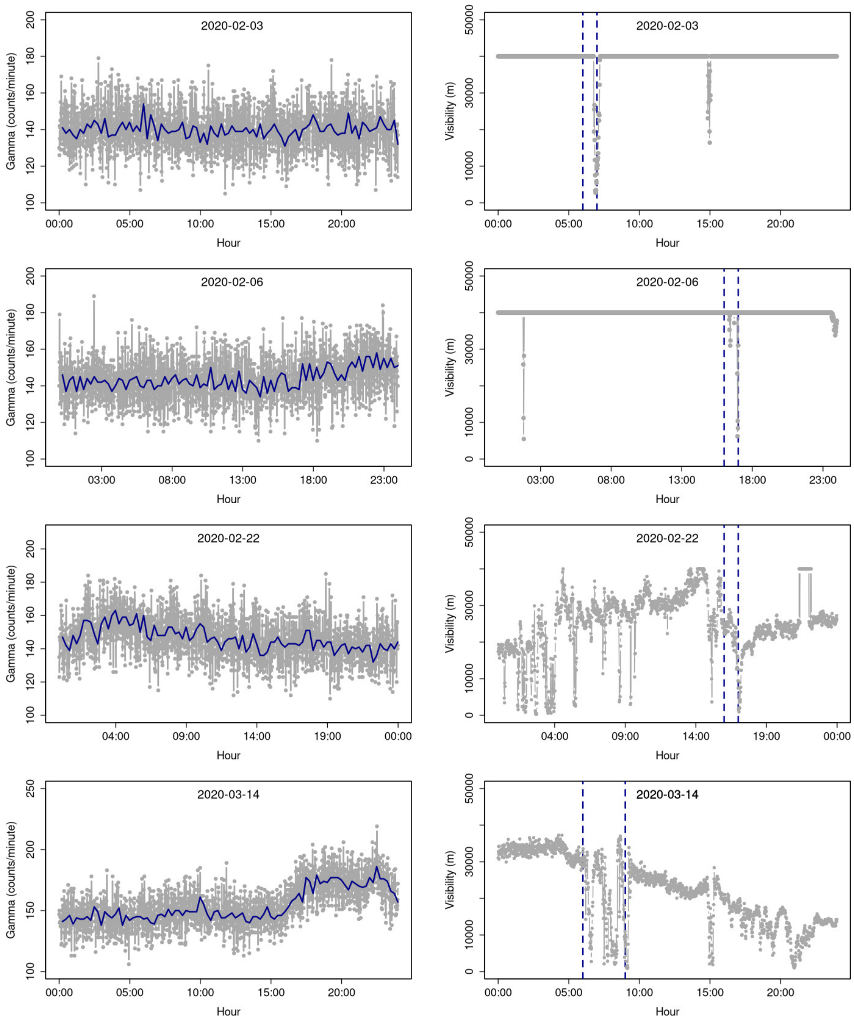

Figure 6. Detail of 1-minute time series of gamma radiation counts (left) and visibility (right) for the days with occurrence of precipitation but no gamma anomalies. The solid (blue) line represents the 15-minute running median of gamma radiation counts. The vertical dashed lines represent the period of occurrence of rain from the available meteorological information.

ibility measurements are very consistent with the qualitative rain data information available. Thus the absence of gamma anomalies (or in two cases - 2020-03/18 and 2020-04-08 - only very small increases barely detectable within the noise level) is not related to eventual errors in the qualitative rain information.

Table 3 shows the % enhancement in gamma radiation and the corresponding distance to the nearest coastline for all days with an anomaly in gamma radiation and/or occurrence of rain. The % enhancement is obtained for each day in which a gamma anomaly was identified by computing the difference of the maximum gamma value relative to the average background value of that day. The distance to the nearest coastline is computed using the Generic Mapping Tools (GMT) software (Wessel et al., 2019) using its low resolution coastline (Wessel & Smith, 1996). Inspection of Table 3, Figure S1, displaying the % increase in gamma radiation as a function of the distance to the nearest coastline and rain characteristics, (and also of the map in Figure 1) doesn't reveal any clear association between gamma radiation anomalies and the type of precipitation as qualita-

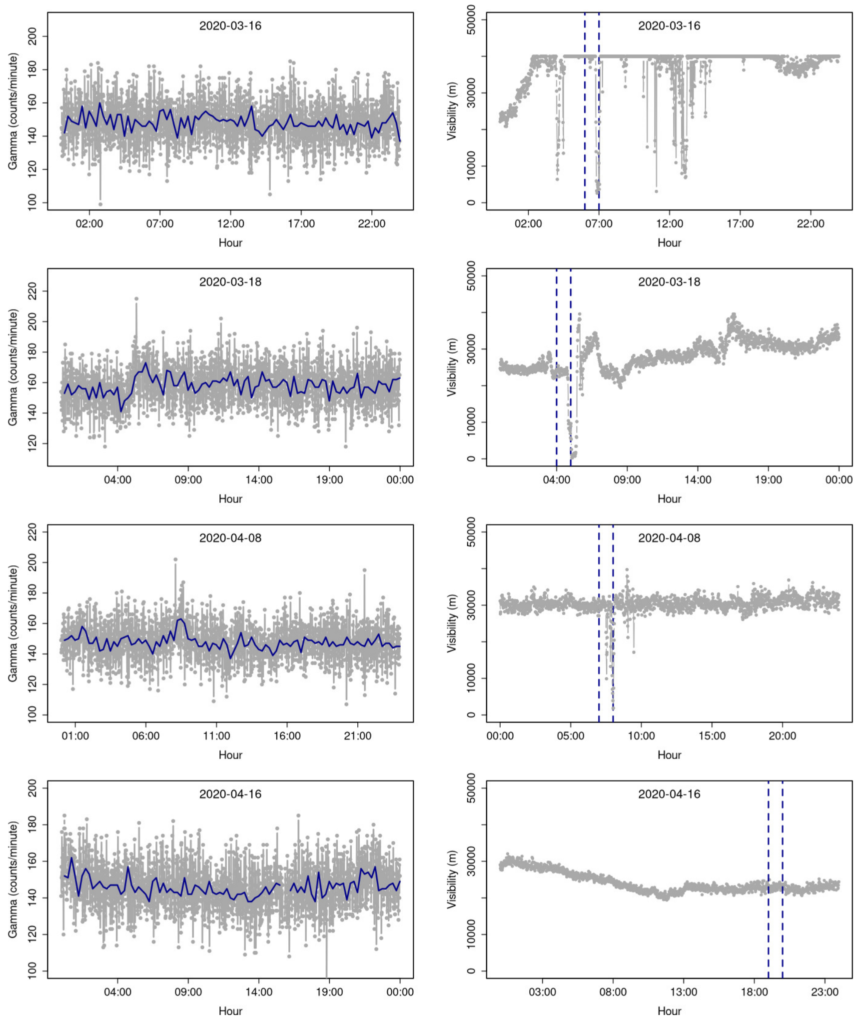

Figure 7. same as in Figure 6.

tively recorded by human observers. Furthermore, no consistent association was observed between the enhancement in gamma radiation and the distance to the nearest landmass.

Table 3. Approximate distance to the nearest coastline for all the days with an anomaly in gamma radiation and/or occurrence of rain. (1) denotes days in which rain is inferred from visibility measurements and (2) rain occurrence suspect (not confirmed by visibility data).

date	rain	increase in gamma (%)	distance to land (km)
2020-01-28	moderate	99	927
2020-01-29	drizzle	33	866
2020-01-30	drizzle	70	849
2020-02-03	drizzle	-	677
2020-02-06	drizzle	-	272
2020-02-18	drizzle	142	118
2020-02-19	(1)	78	112
2020-02-20	(1)	79	81
2020-02-22	drizzle	-	105
2020-03-10	moderate	95	1666
2020-03-14	light/moderate	-	564
2020-03-15	(1)	36	263
2020-03-16	light	-	35
2020-03-18	drizzle	-	649
2020-04-08	light	-	600
2020-04-12	moderate	40	847
2020-04-13	(1)	49	948
2020-04-14	drizzle	54	820
2020-04-16	(2)	-	639
2020-05-09	drizzle	73	213

3.3 Back trajectories

Distance to the coast alone is not an unambiguous criterium to assess continental influences on the marine atmosphere. Air mass back trajectories can be a powerful tool for interpreting fetch behavior, particularly in the absence of local meteorological measurements (e.g. Chambers et al. (2013)). Back trajectories were computed with the HYSPLIT transport and dispersion model (Stein et al., 2015), version 5.2.2, using meteorological information from the Global Data Assimilation System with 1 degree resolution (GDAS1). The 10-day back trajectories were computed at two distinct heights (500m and 2000m) for all the 19 rain events listed in Table 4 (excluding only the 16th April event for which the occurrence of rain is questionable). These heights were chosen to be representative of air masses within, and outside of, the marine boundary layer, respectively.

The back trajectories results are displayed in Figures S2 to S3 and Figure 8 corresponding to 3 distinct cases: i) back trajectories showing no evidence of recent land contact, and for which rainfall does not produce a gamma anomaly (Figure S2); ii) back trajectories showing clear or at least some indication of continental fetch, and for which gamma anomalies are identified (Figure S3); and iii) back trajectories suggesting no recent contact of the air masses with land, but for which rainfall produces rain anomalies (Figure 8). The remaining rainfall event on 2020-03-18 corresponds to a very small gamma anomaly and an air mass with some evidence of land contact. The results are summarized in Table 4. The back trajectories for the rainfall events not associated with a peak in gamma radiation (or a very small anomaly, in the case of the March 18th event), suggest in all those 7 cases no contact with land or at least for the February 22th, March

Table 4. Contingency table for gamma radiation anomalies and land influences derived from 10-days back trajectories.

	land contact	no land contact	
gamma anomaly	6	6	12
no gamma anomaly	0	7	7
	6	13	19

16th and 18th cases no recent land influence (Figure S2). In the case of the 12 rain events with corresponding enhancement in gamma radiation, half of them seem to correspond to air masses with continental influences (Figure S3), while the other half doesn't display evidence of recent land contact (Figure 8). The smallest enhancements in gamma radiation correspond to cases where back trajectories suggest no recent contact of air masses with land, and the largest enhancement corresponds to a location near land, with evident terrestrial influence (Figure 9).

4 Discussion and conclusions

This work documents, for the first time, enhancements of gamma radiation over the ocean associated with the occurrence of precipitation. Most of these enhancements were observed in the southern hemisphere and at varying distances from land, from about 100 km to more than 1500 km to the nearest shoreline.

All the enhancements identified in the marine gamma radiation time series are associated with concurrent occurrence of rain (either explicitly registered by human observation or inferred by visibility data). This fact is consistent with the wet deposition mechanism being the main driver of ground enhancements in gamma radiation.

As it is also the case for gamma radiation enhancements over land, a clear association between the magnitude of the gamma anomaly and the amount and intensity of precipitation is not discernible in this study, although here the analysis is limited by the short length of the time series (5 months), and by the low temporal resolution (1 hour) and the qualitative nature of precipitation observations. Still the information from human observation is in very good agreement with the meteorological optical range measured by the visibility sensor, giving confidence to the use of both types of data.

No systematic relationship is observed between the enhancement in gamma radiation and the distance to land nor the air masses previous contact with land. An obvious limitation to better quantification of such relationships is the small number of events under consideration (12), a longer time series would allow a more detailed assessment.

The back trajectories confirm no recent contact with land in all cases for which rain events do not produce an enhancement in gamma radiation (Figure S2). The oceanic fetch explains why enhancements in gamma radiation are not produced even for comparatively small distances to land (e.g. February 6th and 22nd events). In the 16th March case the distance to land is only 35 km, but the location is very far from continental land masses, near the Tristan da Cunha island in the South Atlantic. This confirms the expected low content of radon progeny in marine air masses away from continental sources.

The gamma radiation enhancements coincident with precipitation events occur, as expected, closer to land (February 18th, 19th 20th events), corresponding to air masses crossing continental regions, or in open ocean, in the tropical Atlantic region, with air masses back trajectories (Figure **??**) suggesting the possibility of continental influences (particularly for the January 29th and 30th cases, not so clear for the 13th April case).

However, gamma radiation anomalies associated with precipitation events are also observed in the open ocean, very far from the coast, and for air masses for which back trajectories don't show evidence of recent contact with land (Figure 8). While in some

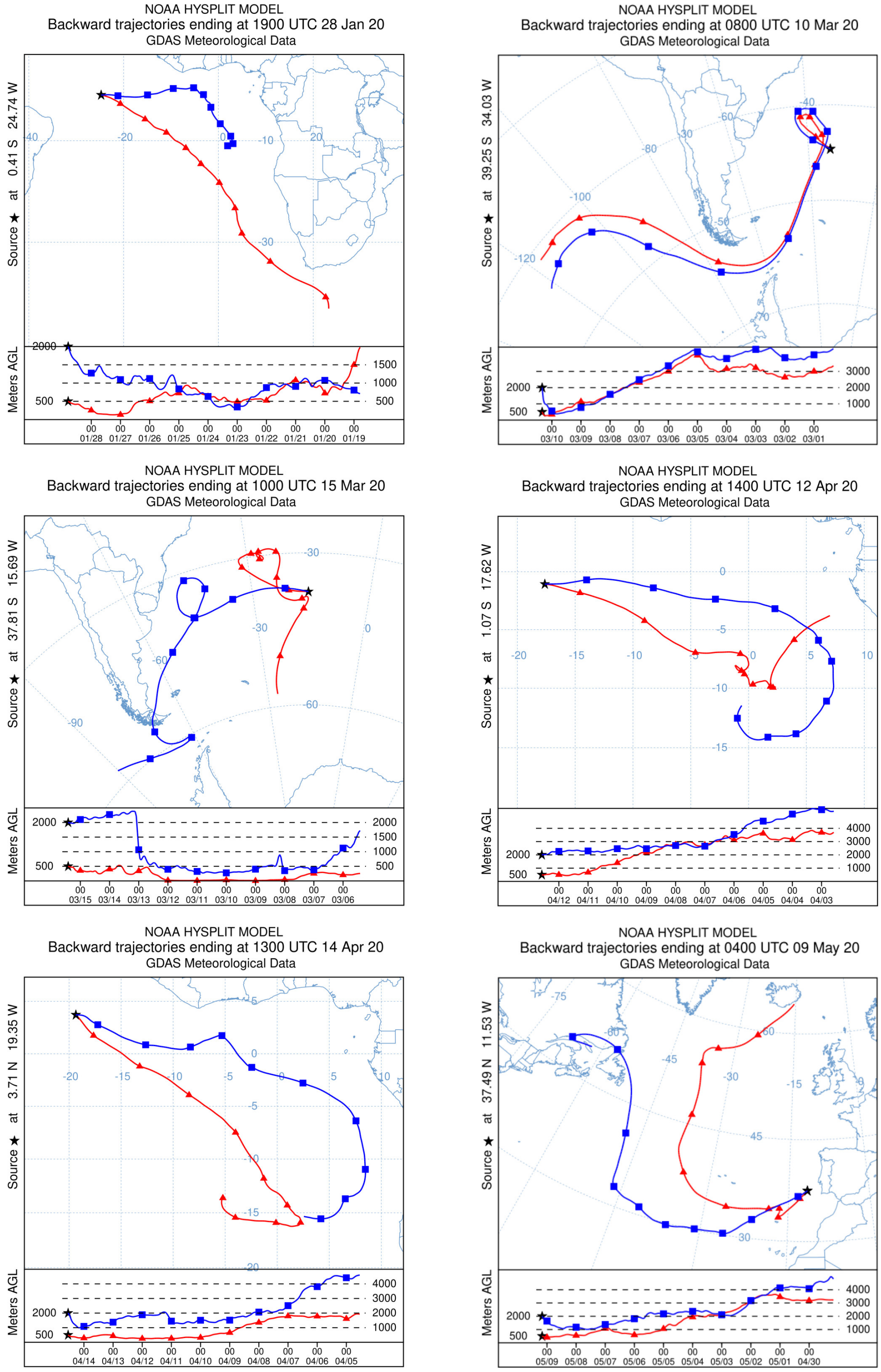

Figure 8. Examples of 10-days back trajectories suggestive of no recent contact with land for the case of rain events with corresponding gamma anomaly.

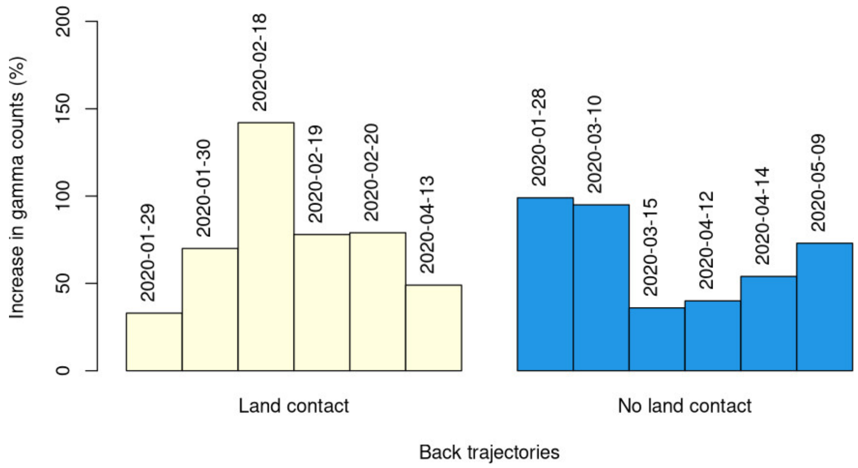

Figure 9. Barplots of the magnitude of the gamma anomalies associated with precipitation for the cases of air masses with recent land contact (left) and no land contact in the previous 10-days (right).

cases (January 28th and March 15th events) limitations in back trajectories can be the culprit - arguably the 28th January trajectory, while not crossing land, is not as different from the 29th and 30th January trajectories - the results show significant enhancements in gamma radiation very far from land and with no evidence of continental fetch from back trajectories results (March 10th, April 12th, April 14th and May 9th). These cases are difficult to explain as resulting only from radionuclides with a predominantly terrestrial source, such as radon and its progeny.

A further potential contribution to these enhancements in gamma radiation observed in open ocean and with no evidence of continental fetch is the gamma-emitting radionuclude Beryllium-7 (Be-7), produced in the Earth's upper atmosphere by cosmic radiation through the spallation of nitrogen and oxygen (Lal, 1967). It has an half-life of $\sim$ 53 days, emitting gamma radiation with energy of $\sim$ 477.6 keV (Tilley et al., 2002). After its formation Be-7 readily becomes associated with aerosols in the sub-micron size range (e.g (Winkler et al., 1998; Ioannidou et al., 2005; Elsässer et al., 2011)) and is then subject to complex horizontal and vertical atmospheric transport processes (Kaste et al., 2002). Precipitation scavenging is the dominant ($\sim$ 90%) process of removal of Be-7 from the atmosphere (Kaste et al., 2002; Kusmierczyk-Michulec et al., 2015; Mohan et al., 2019) and low precipitation rates during drizzles are particularly efficient in scavenging Be-7 by fine droplets (Ioannidou & Papastefanou, 2006).

The cases reported here of gamma radiation enhancements in the open ocean with no apparent continental influences (10th March, 12th and 14th April and May 5th events) correspond according to the back trajectories displayed in Figure 8 to descending air masses. This is consistent with the expectation that concentrations of cosmogenic radionuclides such as Be-7 should increase due to the influx of air from the upper atmosphere enriched in Be-7 radionuclides (Doering & Saey, 2014).

The enhancements in total gamma radiation documented in the present study can't be unequivocally attributed to a specific radionuclide, as the measurements are of total gamma radiation in an energy range (0.475-3 MeV), optimal for radon progeny measurements but also including gamma radiation emitted by Be-7. Thus whether only progeny from airborne radon gas, even if present in small amounts, or other contributions (secondary cosmic radiation, Be-7 radionuclides formed in the upper atmosphere) are responsible for the identified gamma anomalies cannot be settled from the available data. Further measurements would be required, in particular spectral gamma observations which would allow to ascertain which specific elements are contributing to the measured total gamma radiation. An energy-discriminating sensor (Aplin et al., 2017) was actually installed on board NRP Sagres in the framework of the SAIL campaign, but unfortunately mal-functioning of the instrument prevented acquisition of data during the field campaign. In terms of additional measurements direct radon gas concentration observations would be also very helpful, though a detector sensitive enough to be able to measure very low radon concentrations typical of marine air would be necessary (Chambers et al., 2018).

Although the results presented here raise questions that can't be answered without further investigation and collection of new data - a challenging endeavor in a marine setting - the identification of gamma anomalies far from landmasses and apparently not under influence of long-range transport conditions suggests the possibility that not only radon progeny but also other radionuclides, in particular Be-7, can contribute to the identified anomalies in marine gamma radiation. The fact that radon progeny (as well as Be-7) attach rapidly to aerosols after formation, suggests that gamma radiation measurements from pristine, least influenced by land airmasses, could then be used as a proxy of aerosols in the marine environment.

The time series of marine gamma observations (Figure 2, bottom) exhibits larger values and also higher variability in January compared with the observations after February. The coupling between mean and variance is typical of radon progeny time series (S. M. Barbosa et al., 2007), but the fact that very dissimilar background values are observed even at the same location (note the contrast in marine background values at Cape Verde for the two distinct legs of the ship route, at the end of January and then at the end of April) is significant. Possible explanations include synoptic conditions favoring continental fetch during that period and thus increased radon gas concentration and/or seasonal variability of aerosols and wind regime leading to an increase in radon progeny and eventually Be-7 radionuclides. This requires further investigation and a more detailed assessment which is out of scope of the present study focusing on enhancements in gamma radiation associated with precipitation.

Further investigation and additional measurements (energy-discriminating gamma radiation observations and direct radon gas concentration observations) are needed to improve understanding on the sources of ambient radioactivity in the open ocean and assess whether gamma radiation in the marine environment is influenced not only by radionuclides of terrestrial origin, like radon and its progeny, but also cosmogenic radionuclides, like Be-7, formed in the upper atmosphere but with the ability to be transported downward and serve as a tracer of the aerosols to which it attaches. This could complement studies of upper troposphere dust sources and transport based on satellite data (Yang et al., 2022), and would improve understanding on planetary environmental radioactivity and the use of radionuclides as tracers of cloud scavenging and precipitation processes, with implications for the use of radionuclides as tracers of transport and residence time of aerosols in the marine boundary layer.

5 Open Research

Raw measurements from the SAIL campaign are available upon request (S. Barbosa et al., 2021). The datasets of processed measurements used in this manuscript are publicly available: gamma radiation data (S. Barbosa, Almeida, et al., 2022a) and visibility data (S. Barbosa, Almeida, et al., 2022b). The analysis was performed using the R software (R Core Team, 2022). Maps were created with the Generic Mapping Tools (GMT) software (Wessel et al., 2019).

Acknowledgments

The support provided by the NRP Sagres's crew and the Portuguese Navy is gratefully acknowledged. The authors acknowledge the NOAA Air Resources Laboratory (ARL) for the provision of the HYSPLIT transport and dispersion model. Project SAIL received funding from the Portuguese Ministry of Environment and Energy Transition through Fundo Ambiental protocol no 9/2020.

References

Aplin, K. L., Briggs, A. A., Harrison, R. G., & Marlton, G. J. (2017). Measuring ionizing radiation in the atmosphere with a new balloon-borne detector. *Space Weather*, *15*(5), 663–672. Retrieved from `http://dx.doi.org/10.1002/2017SW001610` (2017SW001610) doi: 10.1002/2017SW001610

Balkanski, Y. J., Jacob, D. J., Arimoto, R., & Kritz, M. A. (1992). Distribution of222Rn over the north pacific: Implications for continental influences. *Journal of Atmospheric Chemistry*, *14*(1), 353–374. doi: 10.1007/BF00115244

Barbosa, S., Almeida, C., Amaral, G., Dias, N., Ferreira, A., Camilo, A., & Silva, E. (2022a). *SAIL - gamma radiation data [Dataset].* doi: 10.6084/m9.figshare.20393931.v1

Barbosa, S., Almeida, C., Amaral, G., Dias, N., Ferreira, A., Camilo, A., & Silva, E. (2022b). *SAIL - visibility data [dataset].* doi: 10.6084/m9.figshare.19692394.v2

Barbosa, S., Almeida, C., Guilherme, A., Dias, N., Ferreira, A., et al. (2021). *Raw data collected onboard the sagres ship during the SAIL project campaign [dataset].* INESC TEC research data repository. Retrieved from `https://rdm.inesctec.pt/dataset/nis-2021-003` doi: 10.25747/b2ff-kg31

Barbosa, S., Dias, N., Almeida, C., Amaral, G., et al. (2022). An holistic monitoring system for measurement of the atmospheric electric field over the ocean–the sail campaign. In *Oceans 2022-chennai* (pp. 1–5). doi: 10.1109/OCEANSChennai45887.2022.9775273

Barbosa, S., & Karimova, Y. (2021). *SAIL Data Management Plan.* Zenodo. doi: 10.5281/zenodo.4633444

Barbosa, S., Miranda, P., & Azevedo, E. (2017). Short-term variability of gamma radiation at the {ARM} eastern north atlantic facility (azores). *Journal of Environmental Radioactivity*, *172*, 218-231. doi: 10.1016/j.jenvrad.2017.03.027

Barbosa, S. M., Steinitz, G., Piatibratova, O., Silva, M. E., & Lago, P. (2007). Radon variability at the Elat granite, Israel: Heteroscedasticity and nonlinearity. *Geophysical Research Letters*, *34*, L15309. doi: 10.1029/2007GL030065

Bigg, E. K. (1996). Ion-induced nucleation around radon daughters in remote arctic maritime air. *Tellus B*, *48*(2), 322-328. doi: https://doi.org/10.1034/j.1600-0889.1996.00012.x

Bossew, P., Cinelli, G., Hernández-Ceballos, M., Cernohlawek, N., Gruber, V., Dehandschutter, B., … de Cort, M. (2017). Estimating the terrestrial gamma dose rate by decomposition of the ambient dose equivalent rate. *Journal of Environmental Radioactivity*, *166*, 296–308. doi: 10.1016/j.jenvrad.2016.02.013

Bottardi, C., Albéri, M., Baldoncini, M., Chiarelli, E., Montuschi, M., Raptis, K. G. C., … Mantovani, F. (2020). Rain rate and radon daughters' activity. *Atmospheric Environment*, 117728.

Burnett, J. L., Croudace, I. W., & Warwick, P. E. (2010). Short-lived variations in the background gamma-radiation dose. *Journal of Radiological Protection*, *30*(3), 525.

Chambers, S. D., Preunkert, S., Weller, R., Hong, S.-B., Humphries, R. S., Tositti, L., … Griffiths, A. D. e. a. (2018). Characterizing Atmospheric Transport Pathways to Antarctica and the Remote Southern Ocean Using Radon-222. *Frontiers in Earth Science*, *6*, 190. Retrieved from `https://www.frontiersin.org/article/10.3389/feart.2018.00190` doi: 10.3389/feart.2018.00190

Chambers, S. D., Zahorowski, W., Williams, A. G., Crawford, J., & Griffiths, A. D.

(2013). Identifying tropospheric baseline air masses at Mauna Loa Observatory between 2004 and 2010 using Radon-222 and back trajectories. *Journal of Geophysical Research: Atmospheres*, *118*(2), 992–1004. Retrieved from `http://dx.doi.org/10.1029/2012JD018212` doi: 10.1029/2012JD018212

Cleveland, W., Grosse, E., & Shyu, W. (1992). Local regression models. chapter 8 in statistical models in s (jm chambers and tj hastie eds.), 608 p. *Wadsworth & Brooks/Cole, Pacific Grove, CA.*

Cortes, G., Sempau, J., & Ortega, X. (2001). Automated measurement of radon daughters bi-214 and pb-214 in rainwater. *Nukleonika*, *46*(4), 161–164.

Datar, G., Vichare, G., Raghav, A., Bhaskar, A., Sinha, A. K., & Nair, K. U. (2020). Response of Gamma-Ray Spectrum During Ockhi Cyclone. *Frontiers in Earth Science*, *8*, 15. doi: 10.3389/feart.2020.00015

Doering, C., & Saey, P. (2014). Hadley cell influence on 7be activity concentrations at australian mainland ims radionuclide particulate stations. *Journal of Environmental Radioactivity*, *127*, 88-94. Retrieved from `https://www.sciencedirect.com/science/article/pii/S0265931X13002269` doi: https://doi.org/10.1016/j.jenvrad.2013.10.011

Elsässer, C., Wagenbach, D., Weller, R., Auer, M., Wallner, A., & Christl, M. (2011). Continuous 25-yr aerosol records at coastal antarctica: Part 2: variability of the radionuclides 7be, 10be and 210pb. *Tellus B: Chemical and Physical Meteorology*, *63*(5), 920–934.

European Commission, J. R. C. (2019). *European atlas of natural radiation.* Publication Office of the European Union Luxembourg.

Fisch, A. T. M., Eckley, I. A., & Fearnhead, P. (2022). A linear time method for the detection of collective and point anomalies. *Statistical Analysis and Data Mining: The ASA Data Science Journal*, *15*(4), 494–508. doi: 10.1002/sam.11586

Fujinami, N. (1996). Observational study of the scavenging of radon daughters by precipitation from the atmosphere . *Environment International*, *22, Supplement 1*, 181–185. (The Natural Radiation Environment {VI}) doi: 10.1016/S0160-4120(96)00106-7

Fujitaka, K., Matsumoto, M., Kaiho, K., & Abe, S. (1992). Effect of rain interval on wet deposition of radon daughters. *Radiation Protection Dosimetry*, *45*(1-4), 333–336.

Greenfield, M. B., Domondon, A. T., Tsuchiya, S., Kubo, K., Ikeda, Y., & Tomiyama, M. (2003). Near-ground detection of atmospheric gamma rays associated with lightning. *Journal of Applied Physics*, *93*(3), 1839–1844. doi: 10.1063/1.1536731

Greenfield, M. B., Ito, N., Iwata, A., Kubo, K., Ishigaki, M., & Komura, K. (2008). Determination of rain age via gamma rays from accreted radon progeny. *Journal of Applied Physics*, *104*(7), 074912. doi: 10.1063/1.2990773

Harrison, R. G. (2013). The carnegie curve. *Surveys in Geophysics*, *34*(2), 209–232.

Harrison, R. G. (2020). Behind the curve: a comparison of historical sources for the Carnegie curve of the global atmospheric electric circuit. *History of Geo- and Space Sciences*, *11*(2), 207–213. doi: 10.5194/hgss-11-207-2020

Inomata, Y., Chiba, M., Igarashi, Y., Aoyama, M., & Hirose, K. (2007). Seasonal and spatial variations of enhanced gamma ray dose rates derived from 222Rn progeny during precipitation in Japan . *Atmospheric Environment*, *41*(37), 8043–8057. doi: 10.1016/j.atmosenv.2007.06.046

Ioannidou, A., Manolopoulou, M., & Papastefanou, C. (2005). Temporal changes of 7be and 210pb concentrations in surface air at temperate latitudes (40 n). *Applied Radiation and Isotopes*, *63*(2), 277–284.

Ioannidou, A., & Papastefanou, C. (2006). Precipitation scavenging of 7be and 137cs radionuclides in air. *Journal of Environmental Radioactivity*, *85*(1), 121–136.

Jun, S.-Y., Choi, J., Chambers, S., Oh, M., Park, S.-J., Choi, T., ... Hong, S.-B. (2022). Seasonality of radon-222 near the surface at king sejong station (62°s), antarctic peninsula, and the role of atmospheric circulation based on observations and cam-chem model. *Environmental Research*, *214*, 113998. doi: https://doi.org/10.1016/j.envres.2022.113998

Kaste, J. M., Norton, S. A., & Hess, C. T. (2002, 01). Environmental Chemistry of Beryllium-7. *Reviews in Mineralogy and Geochemistry*, *50*(1), 271-289. Retrieved from https://doi.org/10.2138/rmg.2002.50.6 doi: 10.2138/rmg.2002.50.6

Kusmierczyk-Michulec, J., Gheddou, A., & Nikkinen, M. (2015). Influence of precipitation on 7be concentrations in air as measured by ctbto global monitoring system. *Journal of Environmental Radioactivity*, *144*, 140–151.

Lal, B., D.and Peters. (1967). Cosmic ray produced radioactivity on the earth. In *Kosmische strahlung ii / cosmic rays ii* (pp. 551–612). Berlin, Heidelberg: Springer Berlin Heidelberg. doi: 10.1007/978-3-642-46079-1_7

Livesay, R., Blessinger, C., Guzzardo, T., & Hausladen, P. (2014). Rain-induced increase in background radiation detected by Radiation Portal Monitors. *Journal of Environmental Radioactivity*, *137*(Supplement C), 137–141. doi: 10.1016/j.jenvrad.2014.07.010

Melintescu, A., Chambers, S., Crawford, J., Williams, A., Zorila, B., & Galeriu, D. (2018). Radon-222 related influence on ambient gamma dose. *Journal of Environmental Radioactivity*, *189*, 67–78. doi: 10.1016/j.jenvrad.2018.03.012

Mercier, J.-F., Tracy, B., d'Amours, R., Chagnon, F., Hoffman, I., Korpach, E., ... Ungar, R. (2009). Increased environmental gamma-ray dose rate during precipitation: a strong correlation with contributing air mass . *Journal of Environmental Radioactivity*, *100*(7), 527–533. doi: 10.1016/j.jenvrad.2009.03.002

Mertens, C. J. (2016). Overview of the radiation dosimetry experiment (rad-x) flight mission. *Space Weather*, *14*(11), 921–934.

Mohan, M., D'Souza, R. S., Nayak, S. R., Kamath, S. S., Shetty, T., Kumara, K. S., ... Karunakara, N. (2019). Influence of rainfall on atmospheric deposition fluxes of 7be and 210pb in mangaluru (mangalore) at the southwest coast of india. *Atmospheric Environment*, *202*, 281-295. Retrieved from https://www.sciencedirect.com/science/article/pii/S1352231019300640 doi: https://doi.org/10.1016/j.atmosenv.2019.01.034

Paatero, J. (2000, 02). Wet deposition of radon-222 progeny in northern finland measured with an automatic precipitation gamma analyser. *Radiation Protection Dosimetry*, *87*(4), 273-280. doi: 10.1093/oxfordjournals.rpd.a033008

Paatero, J., & Hatakka, J. (1999). Wet deposition efficiency of short-lived radon-222 progeny in central Finland. *Boreal Env. Res.*, *4*, 285–293.

Paatero, J., Ioannidou, A., Ikonen, J., & Lehto, J. (2017). Aerosol particle size distribution of atmospheric lead-210 in northern finland. *Journal of environmental radioactivity*, *172*, 10–14.

Polian, G., Lambert, G., Ardouin, B., & Jegou, A. (1986). Long-range transport of continental radon in subantarctic and antarctic areas. *Tellus B: Chemical and Physical Meteorology*, *38*(3-4), 178-189. doi: 10.3402/tellusb.v38i3-4.15126

Porstendörfer, J. (2001). Physical parameters and dose factors of the radon and thoron decay products. *Radiation Protection Dosimetry*, *94*(4), 365–373.

Postendorfer, J., Butterweck, G., & Reineking, A. (1994). Daily variation of the radon concentration indoors and outdoors and the influence of meteorological parameters. *Health Physics*, *67*, 283–287.

R Core Team. (2022). R: A language and environment for statistical computing [Computer software manual]. Vienna, Austria. Retrieved from https://www.R-project.org/

Reuveni, Y., Yair, Y., Price, C., & Steinitz, G. (2017). Ground level gamma-ray and electric field enhancements during disturbed weather: Combined signatures from convective clouds, lightning and rain . *Atmospheric Research*, *196*, 142–150. doi: 10.1016/j.atmosres.2017.06.012

Schery, S. D., & Huang, S. (2004). An estimate of the global distribution of radon emissions from the ocean. *Geophysical Research Letters*, *31*(19). Retrieved from https://agupubs.onlinelibrary.wiley.com/doi/abs/10.1029/2004GL021051 doi: 10.1029/2004GL021051

Solomon, K. (1988). Sources of radioactivity in the ocean environment: From low level waste to nuclear powered submarines. *Journal of hazardous Materials*, *18*(3), 255–262.

Stein, A. F., Draxler, R. R., Rolph, G. D., Stunder, B. J. B., Cohen, M. D., & Ngan, F. (2015). NOAA's HYSPLIT Atmospheric Transport and Dispersion Modeling System. *Bulletin of the American Meteorological Society*, *96*(12), 2059–2077. Retrieved from http://dx.doi.org/10.1175/BAMS-D-14-00110.1 doi: 10.1175/BAMS-D-14-00110.1

Takeuchi, N., & Katase, A. (1982). Rainout-Washout Model for Variation of Environmental Gamma-Ray Intensity by Precipitation. *Journal of Nuclear Science and Technology*, *19*(5), 393–409. doi: 10.1080/18811248.1982.9734160

Tilley, D., Cheves, C., Godwin, J., Hale, G., Hofmann, H., Kelley, J., … HR (2002). Energy levels of light nuclei A= 5, 6, 7. *Nuclear Physics A*, *708*(1-2), 3–163.

Wei, Z., Cochran, J. K., Horowitz, E., Fitzgerald, P., Heilbrun, C., Kadko, D., … Landing, W. M. (2022). 210pb and 7be as coupled flux and source tracers for aerosols in the pacific ocean. *Global Biogeochemical Cycles*, *36*(8), e2022GB007378. Retrieved from https://agupubs.onlinelibrary.wiley.com/doi/abs/10.1029/2022GB007378 (e2022GB007378 2022GB007378) doi: https://doi.org/10.1029/2022GB007378

Wessel, P., Luis, J., Uieda, L., Scharroo, R., Wobbe, F., Smith, W. H., & Tian, D. (2019). The generic mapping tools version 6. *Geochemistry, Geophysics, Geosystems*, *20*(11), 5556–5564.

Wessel, P., & Smith, W. H. (1996). A global, self-consistent, hierarchical, high-resolution shoreline database. *Journal of Geophysical Research: Solid Earth*, *101*(B4), 8741–8743.

Whittlestone, S. (1990). Radon daughter disequilibria in the lower marine boundary layer. *Journal of Atmospheric Chemistry*, *11*(1), 27–42. doi: 10.1007/BF00053666

Wilkening, M. (1981). Radon in atmospheric studies: a review..

Wilkening, M., & Clements, W. (1975). Radon 222 from the ocean surface. *Journal of Geophysical Research*, *80*(27), 3828–3830.

Winkler, R., Dietl, F., Frank, G., & Tschiersch, J. (1998). Temporal variation of 7Be and 210Pb size distributions in ambient aerosol. *Atmospheric Environment*, *32*(6), 983–991. Retrieved from https://www.sciencedirect.com/science/article/pii/S1352231097003336 doi: 10.1016/S1352-2310(97)00333-6

Wissmann, F., Dangendorf, V., & Schrewe, U. (2005). Radiation exposure at ground level by secondary cosmic radiation. *Radiation Measurements*, *39*(1), 95–104. Retrieved from http://www.sciencedirect.com/science/article/pii/S1350448704001027 doi: 10.1016/j.radmeas.2004.03.025

Yakovleva, V. S., Nagorsky, P. M., Cherepnev, M. S., Kondratyeva, A. G., & Ryabkina, K. S. (2016). Effect of precipitation on the background levels of the atmospheric beta- and gamma-radiation . *Applied Radiation and Isotopes*, *118*, 190–195. doi: 10.1016/j.apradiso.2016.09.017

Yang, K., Wang, Z., Luo, T., Liu, X., & Wu, M. (2022). Upper troposphere dust belt formation processes vary seasonally and spatially in the Northern Hemisphere. *Communications Earth & Environment*, *3*(1), 24.

Zafrir, H., Haquin, G., Malik, U., Barbosa, S., Piatibratova, O., & Steinitz, G. (2011). Gamma versus alpha sensors for Rn-222 long-term monitoring in geological environments. *Radiation Measurements*, *46*(6-7), 611–620. doi: 10.1016/j.radmeas.2011.04.027

Zahorowski, W., Chambers, S., Wang, T., Kang, C.-H., Uno, I., Poon, S., …

Henderson-Sellers, A. (2005). Radon-222 in boundary layer and free tropospheric continental outflow events at three ace-asia sites. *Tellus B: Chemical and Physical Meteorology*, *57*(2), 124–140.

Zelinskiy, A., Yakovlev, G. A., & Fil'Trov, D. (2021). Relation of gamma dose rate with the intensity of rain showers. *Bulletin KRASEC. Physical and Mathematical Siences*, *36*(3), 189–199.

Zhang, B., Liu, H., Crawford, J. H., Chen, G., Fairlie, T. D., Chambers, S., ... Considine, D. B. e. a. (2021). Simulation of radon-222 with the geos-chem global model: emissions, seasonality, and convective transport. *Atmospheric Chemistry and Physics*, *21*(3), 1861–1887.

Zhang, F., Wang, J., Baskaran, M., Zhong, Q., Wang, Y., Paatero, J., & Du, J. (2021). *Earth System Science Data*, *13*(6), 2963–2994.